# THE FOULING OF ALLOY-800 HEAT EXCHANGER TUBES BY NICKEL FERRITE UNDER BULK BOILING CONDITIONS

**J.L. Cossaboom[1] and D.H. Lister[2]**

[1] Centre for Nuclear Energy Research, 2 Garland Court, Enterprise UNB, Fredericton, NB, Canada, E3B 6C2
jcossabo@unb.ca
[2] Department of Chemical Engineering, University of New Brunswick, PO Box 4400, Fredericton, NB, Canada, E3B 5A3
dlister@unb.ca

## ABSTRACT

A laboratory program at UNB Nuclear is investigating the deposition of corrosion products from cooling water onto heat transfer surfaces. A study of the deposition of nickel ferrite particles from suspension in water at atmospheric pressure onto heated Alloy-800 tubes has been undertaken.

Nickel ferrite particles of a given stoichiometry and two particle sizes – 0.8 μm and 9 μm – were synthesized by solid-state and solution methods, respectively. Their deposition from water under bulk boiling conditions was studied as functions of pH and time. Almost linear deposition with time allowed deposition velocities to be used to characterize the process.

The smaller particles deposited more readily than the larger ones and, for both, maximum deposition occurred when the surface charges on the particles and the test tube were of opposite sign.

A long-term radiotracing experiment allowed particle release processes as well as deposition to be quantified. About seventy percent of the deposit appeared to consolidate and become unavailable for release. A high release coefficient then indicated that the unconsolidated deposit was very labile. Overall, the deposit accumulated up to 300 hours was linear. This behaviour was different from that of magnetite in a previous experiment under similar conditions but with subcooled boiling, suggesting that the mode of heat transfer is important in determining the deposition mechanism.

## INTRODUCTION

Fouling, the accumulation of undesired solid material at phase interfaces, is a phenomenon which is deleterious to a wide variety of industrial operations. The ability to predict and control fouling rates has the potential for significant cost savings.

Particulate fouling is the accumulation of solid particles suspended in a fluid onto a heat transfer surface; it plays an important role in determining the optimum operating conditions and the selection of materials in many systems. The growth of deposits causes a decline in the thermal and hydrodynamic performance of equipment with time by impeding the transfer of heat and increasing the resistance to fluid flow. In addition, if the deposit is thick enough, it can provide an environment for corrosion by the accumulation of aggressive chemicals.

There are reported studies of the mechanisms of deposition of oxide particles of various types onto heat transfer surfaces (Basset et al., 2000 (a); Turner, Lister and Smith, 1990; Turner and Smith, 1992; Turner and Godin, 1994; Charlesworth, 1970; Mizuno, Wada and Iwahori, 1982). It has been postulated that under non-boiling conditions, particle deposition proceeds in two steps occurring in series (Epstein, 1988). The initial step, the transport step, involves the transport of particles from the bulk of the liquid to the vicinity of the surface. This is followed by the attachment step, involving the attachment of particles onto the surface. The deposition rate is related to the rate of particle transport and the rate of particle attachment by the following equation:

$$1/K_d = 1/K_t + 1/K_a \qquad (1)$$

where $K_d$ is the deposition coefficient, $K_t$ is the particle transport coefficient and $K_a$ is the particle attachment coefficient. If one assumes a linear dependence with the concentration in the bulk liquid ($C_b$), the deposition flux ($\Phi_d$) can be expressed mathematically as the product of the bulk concentration times the deposition coefficient (Epstein, 1988).

$$\Phi_d = C_b \cdot K_d \qquad (2)$$

Two classes of surface interaction are considered to be the most important: London-Van-der-Waals attractions and electrical double-layer interactions. The resulting London-Van-der-Waals forces which arise between a particle and a surface are always attractive in a single-phase fluid. For particles with a diameter less than 100 μm, London-Van-der-Waals forces will always dominate over the effect of gravity (Epstein, 1988).

The electrical charges commonly acquired by particles in an electrolyte and the compensating diffuse layer of counter-ions in the liquid adjacent to the particle surfaces give rise to electrical double layer interaction forces that are strongly dependent on the pH of the solution. These forces are attractive when the particle and the wall have unlike charges; the deposition rate will then be mass-transfer controlled:

$$1/K_d \sim 1/K_t \quad (3)$$

If the charge between the particle and wall are the same, the net surface force will be repulsive and the deposition rate will be attachment controlled:

$$1/K_d \sim 1/K_a \quad (4)$$

Therefore a particle will either adhere or be repelled from the surface depending on the forces of attraction and repulsion when a particle is in close proximity to the surface.

Interactions between particles and a liquid result in a thermophoretic particle force when there is a non-uniform temperature environment (Papavergos, 1984). This is the phenomenon whereby small particles in temperature gradients experience a thermal force and consequently move in the direction of the lower temperature. Hence cold walls attract and hot walls repel particles (Kern and Seaton, 1959; McNab and Meisen, 1973). The thermophoretic effect increases with increasing temperature gradient and decreases with increasing particle size. Deposition of particles due to thermophoresis is an effective mechanism for particles less than 2 μm and has been shown to be more important in gases then liquids. Because temperature gradients are small in boiling heat transfer, thermophoretic effects are likely to be small in the experiments reported here and will not be discussed further.

It is well established that there are five steps involved in the fouling of heat transfer surfaces: initiation, transport, attachment, re-entrainment and ageing. Fouling models reported in the literature have primarily focused on the transport, attachment and re-entrainment steps as initiation does not apply to particulate fouling and little is known about how ageing of the deposit affects the overall fouling rate. An extensive investigation of particulate fouling under boiling conditions in high temperature water has been conducted at Chalk River Laboratories. The results have been used to develop a model of particulate fouling that takes account of the transport, attachment, re-entrainment and ageing steps that contribute to the overall fouling process (Turner and Klimas, 2001).

Turner and Klimas (2001) believe that once a particle has been deposited it will be subjected to either re-entrainment or consolidation. The process whereby a particle becomes chemically bonded to either the heat transfer surface or pre-existing deposit is known as consolidation or ageing. The precipitation of dissolved species within the pores of the deposit is the driving force for consolidation while the rate of consolidation is dependent on particle size, the solubility of the deposit, and heat flux. The process of consolidation is irreversible and therefore only unconsolidated deposit is subjected to re-entrainment. The consolidation model for amount of deposited foulant, $m_f$, proposed by Turner and Klimas (2001) is given below:

$$m_f = \frac{K_d C_b}{(\lambda_r + \lambda_c)}\left(t\lambda_c + \frac{\lambda_r}{(\lambda_r + \lambda_c)}\left(1 - e^{-(\lambda_r + \lambda_c)t}\right)\right) \quad (5)$$

where $\lambda_r$ is the removal rate constant and $\lambda_c$ is the consolidation rate constant.

The onset of boiling enhances the particle deposition rate and the contribution to the deposition rate from boiling, $K_b$, can be added to the single phase convective rate to give a deposition rate coefficient for two-phase flow, $K_d$ (2φ), (Turner and Godin, 1994):

$$K_d(2\varphi) = K_d(1\varphi) + K_b \quad (6)$$

where $K_d$ (1φ) is the deposition rate coefficient for single-phase flow and is defined by Eq. (1). However, this approach would appear to be an over-simplification of a complex interaction.

The most commonly invoked mechanism in nucleate boiling is the evaporative mechanism, which relies on the presence of a thin liquid layer at the base of the bubble, the microlayer. During bubble growth, a thin liquid film is on the heater surface beneath the bubble. In sub-cooled boiling, latent heat is removed by evaporation of the film resulting in a temperature decrease below the bubble while the top of the bubble is projected into the cooler bulk liquid resulting in condensation. This simultaneous evaporation and condensation in the bubble is the mass transfer mechanism and was first experimentally verified by Moore and Mesler (1961) who were also the first to observe the presence of a microlayer at the base of a bubble (Robin Jr. and Snyder, 1970). During the initial stages of bubble growth the bubble grows rapidly and the microlayer is formed underneath the bubble. The bubble continues to grow as the liquid evaporates from the microlayer until it totally evaporates and a dry region is formed leaving the solid content of the microlayer to deposit on the surface. In the final stage the bubble reaches a maximum diameter and leaves the heated surface.

Usually, microlayers are supposed to be wedge-shaped in cross-section, increasing in thickness from the center of the bubble. According to Cooper and Lloyd (1969) the microlayers beneath growing bubbles are stagnant and evaporation of the microlayer would cause it to become thinner with time. The microlayer center diminishes with time, accompanied by dry-patch growth, whereas the outer edge increases in thickness with time. This indicates that the microlayer is being replenished by fluid exceeding the rate of liquid evaporation (Jawurek, 1969). As the dry patch in the center of the microlayer grows the particles in

suspension deposit simultaneously. This process was used to explain the concentric-ring deposits that formed on heated surfaces under boiling conditions as reported by several authors (Basset, 1998; Hospeti and Messler, 1965).

The nucleation and growth of bubbles also provide an important mechanism for deposition in that particles can congregate and agglomerate on the bubble's surface and be swept down to its base by interfacial convection currents. Alternatively, depending on the rate of bubble generation and removal, trapped particles may be removed from the vicinity of the solid surface (Basset et al., 2000 (a)).

## EXPERIMENTAL TECHNIQUES

In order to develop a better understanding of the processes involved in the deposition of nickel ferrite it is necessary to have a model system consisting of well defined particles, uniform in size and shape. Therefore model nickel ferrite particles that resemble those present in nuclear reactor plants were synthesized and characterized.

### Solution Synthesis

Particles of non-stoichiometric nickel ferrite were synthesized by following a process involving precipitation from solution followed by oven curing. The synthesis involved the reaction of nickel sulfate with ferrous sulfate in an oxygen-free solution, resulting in the formation of a yellow-green iron and nickel intermediate product mixture. This was then baked in a muffle furnace to form monodispersed particles of non-stoichiometric nickel ferrite with a composition of $Ni_{0.6}Fe_{2.4}O_4$. The average particle size of ~ 9 μm was determined by scanning electron microscopy (SEM), as shown in Figure 1. Two sets of measurements were also performed with a Zeta-meter to determine the point of zero charge (PZC), the pH at which the particle surface has zero net charge, of the nickel ferrite under the following conditions: nickel ferrite suspension concentration of approximately 20 ppm in a potassium nitrate solution of concentration approximately 1 mM. The PZC of the synthesized nickel ferrite was found to occur at a pH of 6.9. Regazzoni and Matijevic (1982) determined the PZC of several different compositions of nickel ferrite under similar conditions. They determined that PZC is independent of stoichiometry over the range $Ni_{0.18}$ to $Ni_{0.79}$; this occurred at a pH of 6.7. Plaza et al. (2001) observed the PZC value of stoichiometric nickel ferrite to occur within the pH range of 6.6 - 6.8.

### Solid-State Synthesis

Colloidal particles of nickel ferrite were synthesized with several solid-state preparations using different starting reagents. The preparations were the reaction of: hematite with nickel oxide; maghemite with nickel oxide; and, nickel carbonate with hematite. For experimental comparison purposes, nickel ferrite of the same composition as that obtained in the solution synthesis but with a different particle size was required. Non-stoichiometric nickel ferrite was obtained by mixing the appropriate quantity of magnetite with each of the above preparations to incorporate $Fe^{2+}$ into the nickel ferrite lattice. The resulting nickel ferrite particles were monodispersed, colloidal (~0.8 μm) and nearly spherical in shape, as shown in Figure 2. The PZC was determined to occur at a pH of 6.6, consistent with that reported by Regazzoni and Matijevic (1982) and Plaza et al. (2001), as mentioned above.

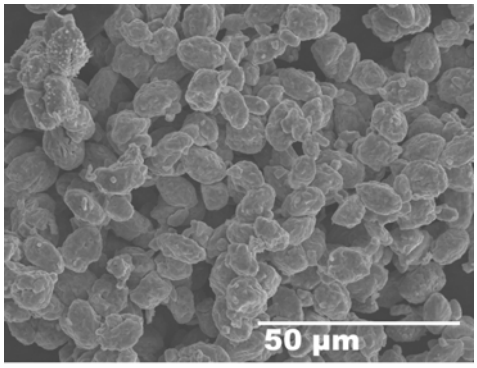


Fig. 1 SEM of Solution Synthesized Nickel Ferrite Particles

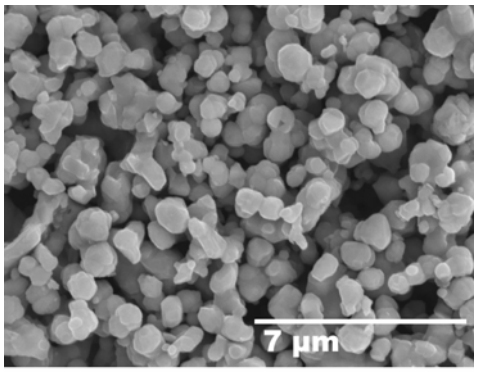


Fig. 2 SEM of Solid-State Synthesized Nickel Ferrite Particles

### Deposition Experiments

Nickel ferrite was added to the coolant of a recirculating water loop that is primarily constructed of stainless steel but has a vertical glass test section. The loop operates at atmospheric pressure and at temperatures up to 96˚C. The test section is a 1.5 m-long glass column with an inner diameter of 9.93 cm. The gasketed plate closure at the top of the test section contains two outlet ports and a port for the insertion and removal of the section of Alloy-800 steam generator tube, which is used as the heat transfer test surface. The Alloy-800 tube is 30 cm long with a diameter of 1.59 cm and is equipped with a 25 cm-long cartridge

heater capable of generating a maximum heat flux of 240 kW/m$^2$. To ensure a smooth up-flow around the heater tube, its end is made of a plug of stainless steel 304, machined with a parabolic profile, that is brazed into position. The loop contains two 170 L tanks, each equipped with a Caloritec heater, mechanical stirrer and a nitrogen gas purging system. A small heat exchanger is installed after the test section to remove heat added to the coolant by the boiler tube and a stainless steel centrifugal pump provides the flow for the system.

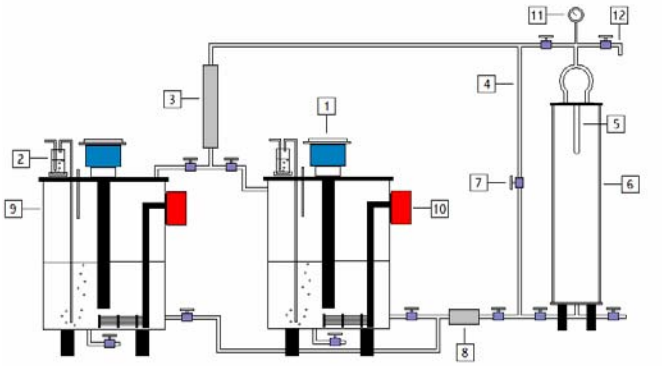


Fig. 3 Experimental Recirculating Loop

During an experimental run, a sample of coolant was taken every hour from a sample line located at the top of the loop just downstream of the test section. It was analyzed for pH and nickel ferrite concentration via either atomic absorption spectrometry (AA) or UV-visible spectrophotometry. Adjustments to the pH were made with potassium hydroxide or nitric acid as required. Air was excluded from the system via continuous purging with nitrogen for the duration of the experiment and for 24 hours prior to the addition of nickel ferrite. The concentration of nickel ferrite particles was maintained at 5 ppm for all experiments except the latter half of the radiotracing experiment when it was doubled.

Upon the stabilization of the nickel ferrite concentration, the temperature and the pH in the loop, the test section was by-passed to allow for the insertion of the Alloy-800 tube. The tube was introduced into the test section, switched on, and the experiment begun for the desired time. All experiments were conducted at 96˚C with a heat flux of 240 kW/m$^2$. The amount of deposit was measured by removing the Alloy-800 tube and scraping off all the deposit with a glass rod fitted with a rubber end; concentrated hydrochloric acid (HCl) was used to remove remaining material from the scraped area. The deposit was completely dissolved in HCl and analyzed with AA spectrometry or UV-visible spectrophotometry.

For the experiments on the two particle sizes at different pH values, deposition was measured at times up to 24 hours. Deposition velocity was estimated for each experiment by taking the mass of deposit per unit surface area at 10 hours and dividing by the time and bulk concentration. This assumes that deposition is effectively linear over the first few hours.

**Radiotracing Experiment**

The loop was also used to determine the deposition of nickel ferrite particles under bulk boiling conditions as a function of time by an on-line radiotracing technique. Due to the long (92 years) half-life of $^{63}$Ni, which decays with the emission of a beta particle and is not useful for radiotracing, it was decided to irradiate the magnetite starting material and not the final nickel ferrite product. The irradiated magnetite would then be used in the synthesis, resulting in particles of nickel ferrite containing radioactive $^{59}$Fe with a half-life of 44.6 days.

Two samples, approximately 7 g each, of magnetite were irradiated for 10 hours in the McMaster University Research reactor to produce $^{59}$Fe, a useful gamma emitter, by the neutron activation of $^{58}$Fe. These samples were then used in the preparation of nickel ferrite by the reaction of hematite and nickel oxide. The magnetite, it will be recalled, produces the non-stoichometric version of nickel ferrite. The radioactive sample of nickel ferrite, 16 g of monodispersed particles 0.8 μm in diameter, was then mixed with 44 g of non-radioactive nickel ferrite of the same particle size and added to 11 L of deionized water in a small shielded reservoir. Additions of the radioactive nickel ferrite solution from the reservoir were added to the re-circulating loop radioactive tank as required via a peristaltic pump.

The activity of deposited $^{59}$Fe was monitored on-line by measuring the intensity of the gamma rays at 1095 keV with a germanium gamma detector positioned in front of the Alloy-800 tube. This allowed the build-up of nickel ferrite on the tube to be determined. The detector was calibrated using a radioactive source of $^{60}$Co and $^{137}$Cs of known intensity. The intensity of the gamma rays emitted was measured every half an hour and the data were analyzed with a Canberra S100 Multi-Channel Analyzer. To minimize the effects of background radiation the head of the detector was shielded with lead bricks. A small window, 2.5 cm by 0.7 cm, in a lead brick positioned in front of the detector and in line with the vertical axis of the tube, allowed for the observation of a portion of the tube, approximately 23 cm$^2$. The window was also aligned vertically to allow the maximum amount of tube to be observed by the detector while minimizing the amount of

coolant observed, thereby minimizing the background. At the end of the experiment radioactive deposit was scraped and dissolved off the test section in three circumferential rings at the bottom, middle and top and all of it dissolved in HCl. Therefore a determination of the radioactivity of the solution then provided an average area concentration of deposit.

The radiation background was determined while the radioactive suspension of nickel ferrite was present in the flowing coolant prior to the insertion of the Alloy-800 tube. In addition, the background radiation was measured at the completion of the experiment after the fouled tube had been removed and the radioactive suspension was still present in the flowing coolant. This allowed the background radiation build-up to be determined pro-rata to the subsequent measured build-up on the tube. In other words it was assumed that the background followed the same development as the experimental data. The radioactive build-up on the Alloy-800 tube was then determined by subtracting the background from the experimental data.

The experimental run began with the radioactive nickel ferrite suspension at a concentration of 5 ppm and a coolant pH and temperature of 7.5 and 96˚C, respectively. After 293 hours the source was switched to the non-radioactive suspension, 5 ppm, by valving in the second tank and valving out the first tank. This indicated any mechanism involving the release of material from the surface, as the radioactivity on the tube would decrease if particle release were an active mechanism. The source was then switched back to the radioactive suspension at a different concentration, 10 ppm, after 415 hours. The concentration of the suspended nickel ferrite in the coolant was continuously monitored by regularly taking samples and dissolving the suspended particles in hydrochloric acid followed by analysis via atomic absorption or UV-visible spectrophotometry. In addition, the specific activity of the nickel ferrite in suspension was continuously monitored by sampling the circulating coolant. At the completion of the experiment the tube was removed from the glass test section.

## EXPERIMENTAL RESULTS

### Effect of Time on Deposition in Boiling

A set of experiments was performed to determine the effect of time on deposition of non-radioactive nickel ferrite onto the Alloy-800 heat exchanger tube under bulk boiling conditions (see Figure 4). All runs were performed under the same experimental conditions with only the duration of the run varying. The concentration and $pH_{30^{\circ}C}$ of the loop were maintained at 5 ppm and 7 respectively.

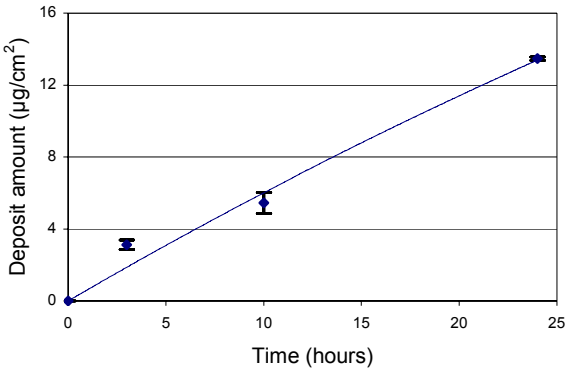


Fig. 4 Effect of Time: Deposition vs. Time for Solution-Synthesized Nickel Ferrite, 9 µm Diameter

### Effect of pH on Nickel Ferrite Deposition

Experimental runs were performed on non-radioactive nickel ferrite particles of both sizes to determine the effect of pH on deposition. Each set of runs was performed under the same experimental conditions while only one parameter varied, the pH. In each run, the pH of the coolant was set with potassium hydroxide (KOH) and nitric acid ($HNO_3$) solutions and varied from approximately 3.3 to 10.0. The effect of the coolant chemistry on deposition for a particle diameter of 9 µm and for 0.8 µm is given in Figures 5 and 6 respectively.

### Radiotracing Deposition Experiment

A radiotracing deposition experiment was performed while only the radioactivity of the circulating coolant and concentration of the active nickel ferrite in the reservoir tank varied. In the radiotracing deposition experiment the intensity of the gamma ray at 1095keV from $^{59}Fe$ was recorded every half an hour. The experiment began with the insertion of the tube into the recirculation loop and after 293 hours the source was switched from a suspension of radioactive nickel ferrite, with a concentration of 5 ppm, to a suspension of non-radioactive nickel ferrite at a concentration of 5 ppm. As a result, the activity on the tube decreased. At approximately 415 hours the source was then switched back to a suspension of radioactive nickel ferrite at a concentration of 10 ppm. As a result, the activity on the tube increased again as expected. Figure 7 shows the build-up of radioactivity on the tube, corrected for background, as a function of time; it also contains a model fit, described later.

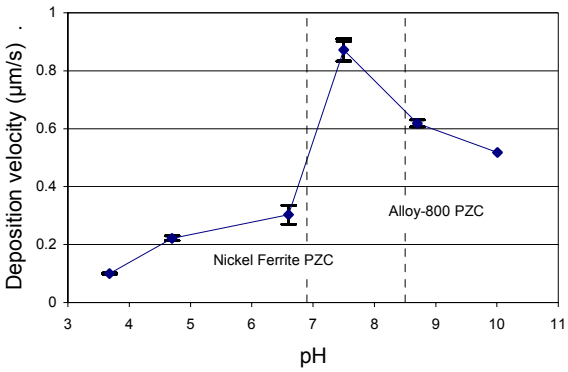


Fig. 5 Effect of pH ($d_p$ ~ 9 µm): Deposition Velocity vs. pH

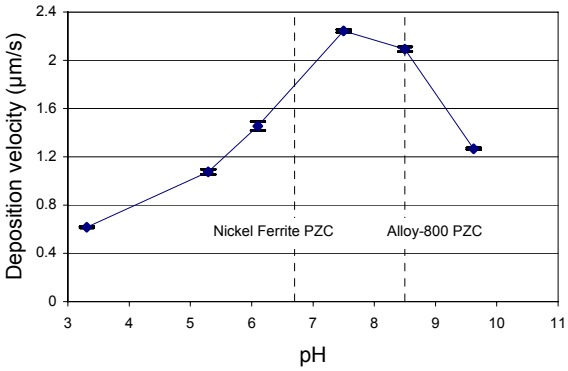


Fig. 6 Effect of pH ($d_p$ ~ 0.8 µm): Deposition Velocity vs. pH

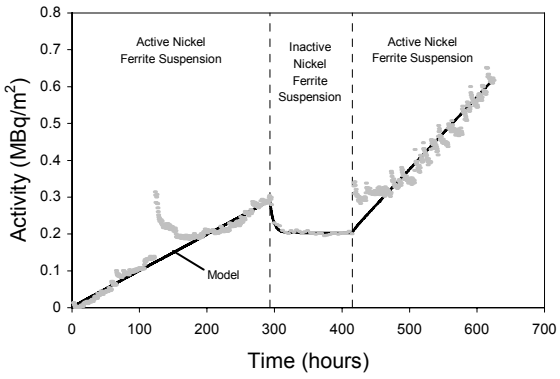


Fig. 7 Radiotracing Experiment: Radioactive Nickel Ferrite Build-up versus Time ($d_p$ ~ 0.8 µm)

Particle removal was shown to be an active mechanism in the fouling process since the switch to the inactive nickel ferrite source caused a decrease in the surface activity of the tube. If removal were a negligible process the activity on the tube would have remained constant after the switch to the inactive nickel ferrite source. Even though the surface activity decreased, the mass of nickel ferrite deposited would have continued to increase – presumably following an extrapolation of the first section of Figure 7 before 293 hours. The activity of nickel ferrite per unit volume in suspension was monitored during the run by frequently taking samples of the coolant and analyzing for nickel ferrite concentration (Figure 8).

The activity of the coolant was nominally constant prior to the nickel ferrite source switch at 293 hours except for a concentration burst which occurred at approximately 120 to 170 hours. This burst was due to the disturbance of settled particles in the radioactive tank after an adjustment to the pH of the coolant. After the nickel ferrite source switch from radioactive to non-radioactive at 293 hours the activity of nickel ferrite per unit volume in suspension decreased, eventually leveling off. At 415 hours the nickel ferrite source was switched back to the radioactive source resulting in a concentration burst followed by fluctuations in the activity. Once again the concentration burst was due to the disturbance of settled particles in the radioactive tank. However, the fluctuations in the activity directly resulted from fluctuations in the coolant concentration. Upon the source switch at 415 hours the nickel ferrite concentration was increased to a nominal 10 ppm but was difficult to maintain.

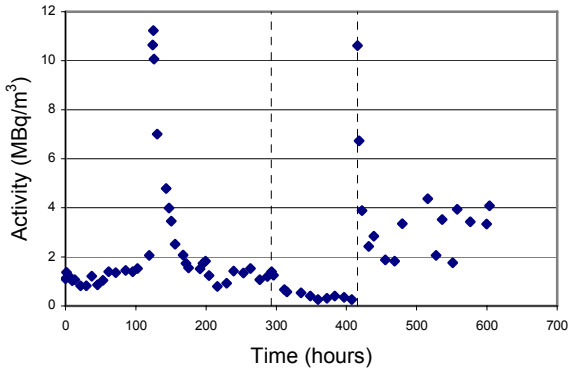


Fig. 8 Activity of Nickel Ferrite per Unit Volume in Suspension versus Time ($d_p$ ~ 0.8 µm)

## DISCUSSION

### Effect of Time on Deposition in Boiling

For times up to about 25 hours the mass of nickel ferrite deposited onto the Alloy-800 tube surface was shown to increase at an almost constant rate, as shown in Figure 4. This behaviour is similar to that seen by other authors for the deposition of various corrosion products under boiling conditions. McCrea (2001) observed a linear dependence for the deposition of magnetite particles onto an Alloy-800

surface, which is consistent with that previously reported (Charlesworth, 1970; Turner and Smith, 1992; Turner and Godin, 1994). Mizuno et al. (1982) observed a similar trend for the deposition of suspended hematite particles onto a boiling heat transfer surface. The same linear trend has been reported for isothermal and subcooled boiling conditions (Turner, Lister and Smith, 1990; Basset, 1998).

This constant increase with respect to time indicated that net removal was negligible during the rather short time frame studied. If the removal of particles from the surface were an active mechanism the deposition amount would begin to level off and the rate of deposition and removal might reach a state of equilibrium, exhibiting asymptotic behavior. According to Charlesworth (1970), for the deposition of magnetite at 285˚C and 6.9 MPa, the time required to reach a state of equilibrium is 100 hours of operation. However, in these experiments with nickel ferrite, equilibrium was not reached after 300 hours of deposition (see Figure 7).

**Effect of pH on Nickel Ferrite Deposition**

The deposition velocities of nickel ferrite from suspension onto an Alloy-800 tube for particle sizes of 9 μm and 0.8 μm are shown in Figures 5 and 6 respectively. The deposition velocity reaches a maximum at a pH value between 7.5 and 8.0 for both sizes of particle. This point of maximum deposition is in good agreement with the results obtained for magnetite deposition under isothermal and sub-cooled boiling conditions (Turner, Lister and Smith, 1990; Basset, 1998), but is not in agreement with that reported for magnetite deposition under bulk boiling conditions (McCrea, 2001). McCrea (2001) reported that the deposition velocity reaches a maximum at a pH of approximately 5.0.

It can be concluded that coolant chemistry has an important influence on the deposition rate, since the charge on both the Alloy-800 tube and the nickel ferrite particles can be changed by adjusting the pH of the coolant. In fact, it is well-known that high rates of deposition are attained at system pHs between the PZC values of the surface and the particles (Turner and Smith, 1992; Turner, Lister and Smith, 1990). This occurs due to a modification of the characteristics of the surface charge and, hence, the electric double layer interactions. The charge on the surface of the Alloy-800 tube or nickel ferrite particles is determined by the difference between the coolant pH and the PZC of the corresponding surface. When the coolant pH is equal to the pH value corresponding to the PZC of the surface it will have no net charge. However, if the coolant pH is greater than the PZC the surface will have a negative charge whereas if the pH is less than the PZC the surface will possess a positive charge.

The PZC for the Alloy-800 was assumed to occur at a pH of approximately 8.5 (Turner, Lister and Smith, 1990) while the PZC of the nickel ferrite particles was determined to occur at pHs of 6.9 and 6.7 for the 9 μm and 0.8 μm particles, respectively. The above theory resulted in the development of the following conclusions to describe how the coolant pH affects nickel ferrite deposition.

When the coolant pH lies between the PZC of the tube and particle surfaces, those surfaces possess a positive and negative charge respectively. In this pH range an attractive force will exist and deposition will be favoured. However, when the coolant pH lies outside of this range a repulsive force will exist as the surfaces will possess the same charge and deposition will be unfavourable.

It was also observed that the deposition occurs at a greater rate in basic conditions than acidic conditions as shown in Figures 5 and 6. This trend was also observed for magnetite under isothermal and sub-cooled boiling conditions (Turner, Lister and Smith, 1990; Basset, 1998). It suggests that the repulsive force between the nickel ferrite particles and the Alloy-800 surface is weaker under basic conditions than acidic conditions.

**Effect of Particle Size on Nickel Ferrite Deposition**

By comparison of Figures 5 and 6 it is seen that the deposition velocity and hence the amount of nickel ferrite deposited is 2.5 times larger for the 0.8 μm particles than for the 9 μm particles. For a pH between the PZCs of the particle and tube surfaces an attractive force exists. Within this range deposition is favoured and the deposition rate will be transport controlled. According to Beal (1970), in single-phase flow the deposition of sub-micrometer particles is entirely diffusion controlled and the deposition rate decreases with increasing particle size. For particles greater than the sub-micrometer range, however, momentum effects become increasingly important and eventually dominate the transport of larger particles. This results in much higher deposition rates for larger particles.

It is suggested that in two-phase flow there are two major mechanisms: a diffusion term, as illustrated by Beal, and a boiling term. However, since the deposition rate of the 9 μm particles is smaller than the deposition rate of the 0.8 μm particles it is believed that the boiling term is the more dominant of the two mechanisms. The boiling term affects the transport of the particles to the surface by disturbing the boundary layer and therefore the diffusion process and by trapping the particles with bubbles via the mechanism described earlier.

The 0.8 μm nickel ferrite particles fall within the diffusion regime where it is well known that particles are transported to the heat transfer surface via turbulent eddies. However, boiling affects the transport of these particles to the surface by disturbing the boundary layer and therefore

the diffusion process. Turbulence within the boundary layer increases, resulting in more turbulent eddies available for particle transport, thereby increasing the amount deposited.

As previously described, Basset (1998) observed that magnetite particles can congregate and agglomerate on a bubble's surface and be swept down to its base by interfacial convection currents. Alternatively, depending on the rate of bubble generation and removal, trapped particles may be removed from the vicinity of the surface. In addition to the collection of magnetite particles on the bubble surface, Basset et al. (2000 (b)) observed ring-shaped deposits at the bubble nucleation sites. Therefore, it is believed that this phenomenon was present in these nickel ferrite deposition experiments, as ring-shaped deposits were also observed at the bubble nucleation sites. As previously stated, boiling results in more turbulent eddies available for the transport of the 0.8 μm particles to the heat transfer surface, thereby increasing the quantity of nickel ferrite particles collected on the bubble's surface. These particles congregate and agglomerate on the bubble's surface and are easily swept to the base of the bubble via interfacial convective currents due to their small size. The same procedure whereby particles are trapped and agglomerate on the bubble's surface occurs for the larger 9 μm particles; however, due to their larger size or weight the rate of transfer of these particles to the base of the bubble is believed to be smaller than the rate of bubble generation and removal, thereby resulting in the larger trapped particles being removed from the vicinity of the solid surface via the departing bubbles. By contrast, once the smaller 0.8 μm particles are trapped on the bubble's surface they agglomerate and are transported down to the base of the bubble prior to the departure of the bubble, resulting in the ring-shaped deposits that were observed by Basset et al. (2000 (b)) for the deposition of magnetite. Thus, the interplay of these processes, diffusion and boiling, are believed to be responsible for the higher deposition rate of the smaller nickel ferrite particles.

**Radiotracing Experiment**

Particle removal was shown to be an active mechanism in the fouling process, for in the radiotracing experiment the switch to the inactive nickel ferrite source caused a decrease in the surface activity of the tube (see Figure 7). The rate of that decrease for nickel ferrite was larger than that for magnetite (Basset, 1998).

Upon switching to the inactive source at 293 hours the activity on the tube rapidly dropped before leveling off to a constant value. As can be seen in Figure 8, the activity of the coolant decreased after the switch but never reached zero; therefore there was a residual amount of radioactive suspension available in the coolant for deposition. A rapid decrease was also observed after the concentration burst that occurred at 120 to 170 hours, while rapid decreases occurred after the random concentration spikes that occurred following the valve-in of active coolant at 415 hours.

After the second switch at 415 hours from the inactive to active source the tube activity began generally to increase again. However, the concentration was maintained at a value nominally double that before the switch, 10 ppm versus 5 ppm, on average. From a comparison of the rates of increase in activity during both the active deposition sections of Figure 7 it can be deduced that the mass of nickel ferrite increases linearly with increasing concentration, since the rates of change in activity or slopes of the two sections are $2.78\times10^{-7}$ MBq/m$^2$s and $5.49\times10^{-7}$ MBq/m$^2$s, that is, the rate approximately doubled.

As shown in Figure 7, when the coolant was maintained at a concentration of 5 ppm up to 415 hours, the activity buildup followed a relatively smooth curve with few concentration spikes. However, after 415 hours, the coolant was maintained at 10 ppm and the activity followed an irregular buildup that resulted in spikes in the activity. This occurred because it proved to be difficult to maintain the concentration at 10 ppm; small fluctuations in the coolant concentration resulted. The concentration continually needed large adjustments by the addition of active nickel ferrite to the tank whereas prior to 415 hours the concentration was continually monitored but adjustments were less drastic and less frequent. These larger adjustments to the concentration caused the activity on the tube to increase followed by rapid releases, thereby resulting in activity spikes. This trend was repeated for the remainder of the experiment. It was determined that the rates of decrease of activity after the spikes were of the same order of magnitude and were comparable with those of the rapid releases that occurred at approximately 120, 290 and 415 hours.

Under sub-cooled boiling conditions with magnetite, Basset (1998) found excellent agreement between his experimental radiotracing data and the Kern and Seaton Model (1959). Therefore, this model was examined for possible application to these experimental results. The Kern and Seaton model gives the following relation:

$$\frac{dm_f}{dt} = K_d C_b - k_r m_f \tag{7}$$

where $k_r$ is the release coefficient. When the activity of the nickel ferrite suspension is designated by $A_{sol}$ and $A_t$ represents the activity on the tube, Equation 7 becomes:

$$\frac{dA_t}{dt} = K_d A_{sol} - k_r A_t \tag{8}$$

It will be obvious, however, that this simple first order approach cannot describe the pattern of deposition and release shown in Figure 7. The rapid release after the flow switch at 293 hours would require a release coefficient, $k_r$, that would be high enough to cause a leveling-off of the data curve during the deposition periods. The deposition curves however, are overall almost linear. Moreover, the fact that only a portion of the deposited activity is released after the flow switch, with the data leveling-off at about 70% of the value just before the switch, suggests that a process of deposit consolidation occurs (it should be noted that the residual coolant activity during the exposure to nominally inactive coolant between 293 and 415 hours was too low to account for the final deposition activity at 415 hours).

The 30% labile, or unconsolidated, portion of the deposit is apparently released with a first order release coefficient $k_r$ of $5.0\times10^{-5}$ $s^{-1}$; the fit of this release model to the data between 293 hours and 415 hours is indicated in Figure 7. It should be noted that the reductions in surface activity after the "spikes", which are coincident with the spikes in the bulk concentration of activity as shown in Figure 8, follow similar release kinetics.

Although the simple first order model fits the release portion of the activity build-up curve very well, the depositing portions are not amenable to the Kern-Seaton approach. Thus, a 30% labile portion of the deposit with a release coefficient of $5.0\times10^{-5}$ $s^{-1}$ cannot be reconciled with the roughly linear build-up (if the spikes are neglected) in the periods before 293 hours and after 415 hours. Furthermore, the leveling-off of the data in the release period at a constant value suggests that the residual bulk activity in that period caused no concomitant deposition. Nevertheless, the data in the build-up periods are self-consistent in that the average linear rate in the second is about twice that in the first, corresponding to the doubling of the average bulk activity from 1.3 $MBq/m^3$ in the first period to 2.6 $MBq/m^3$ the second period. This linear deposition model, which is also shown in Figure 7, produces deposition velocities in the first and second periods of $2.14\times10^{-7}$ m/s and $2.11\times10^{-7}$ m/s, respectively.,

It is interesting to compare these results with those obtained from magnetite at similar chemistry conditions of pH 7.5 (Basset et al., 2000 (b)). There, the excellent fit of the simple first-order model to the radiotracing data for magnetite produced a $k_d$ of $3.8\text{x}10^{-7}$ m/s and a $k_r$ of $3.7\text{x}10^{-6}$ $s^{-1}$. That deposition constant is in reasonable agreement with the average value of $2.13\times10^{-7}$ m/s from this experiment with nickel ferrite, even though the mode of heat transfer with magnetite was sub-cooled boiling as opposed to bulk boiling here. The reason for the rather low value for radiotraced nickel ferrite particles of 0.8 μm particle size compared with the deposition velocities in Figure 6 is not clear, though it may be associated with the surface averaging technique in the radiotracing experiment as opposed to the complete surface measurement technique in the other experiments.

The high release coefficient for the radiotraced nickel ferrite is also noteworthy; it indicates that the unconsolidated portion of the deposit is very labile. This may reflect a difference in mechanism between the release process in sub-cooled boiling (as in the magnetite experiment) and that in bulk boiling. The different heat transfer mechanism may also be responsible for the deposit consolidation with nickel ferrite.

## CONCLUSIONS

Under bulk boiling conditions, the amount of nickel ferrite deposited onto a heated Alloy-800 tube increased almost linearly with time. Release of particles from the surface was shown to be small during the 10 hours taken to establish a deposition velocity.

The deposition rate of nickel ferrite particles of both sizes onto Alloy-800 tubing under bulk boiling conditions was a maximum at a pH between 7.5 to 8.0, when the particles and the surface posses opposite electrostatic charges. This range of maximum deposition for nickel ferrite under bulk boiling was in agreement with the range of maximum deposition for magnetite (determined in earlier experiments) under isothermal and subcooled boiling conditions. However it was not in agreement with magnetite deposition under bulk boiling conditions.

The deposition rate of sub-micrometre nickel ferrite particles was greater than that of large (up to 10 μm) particles. This difference was attributed to the effect of boiling on the transport of particles to the surface.

A radiotracing experiment confirmed that release and deposition of 0.8 μm particles occurred under the conditions of bulk boiling at pH 7. However, unlike the data for magnetite in a similar experiment under sub-cooled boiling conditions, in which a straightforward model invoking first-order deposition and release coefficients described the data very well, the nickel ferrite data suggested that consolidation of 70% of the deposit had to be taken into account. Moverover, the rapid release to the coolant of the 30% labile portion of the deposit, which displayed first-order kinetics, apparently did not take place concomitantly with deposition, since total accumulation on the surface was almost linear. .

## NOMENCLATURE

$A_{sol}$ activity of the nickel ferrite suspension, $Bq/m^3$
$A_t$ activity of the total deposit on the Alloy-800 tube, $Bq/m^2$
$C_b$ bulk concentration, $kg/m^3$
$k_d$ particle deposition coefficient, m/s

$k_r$ removal constant, $s^{-1}$
$K_a$ particle attachment coefficient, m/s
$K_b$ deposition rate from boiling, m/s
$K_d$ or $K_d$ (1φ)deposition velocity, m/s
$K_d$ (2φ) two-phase flow deposition coefficient, m/s
$K_t$ particle transport coefficient, m/s
$m_f$ mass of fouling material per unit area, $kg/m^2$
$\lambda_c$ consolidation rate constant, $s^{-1}$
$\lambda_r$ removal rate constant, $s^{-1}$
$\Phi_d$ particle deposition flux, $kg/(m^2 \cdot s)$

**ACKNOWLEDGEMENT**

The Natural Sciences and Engineering Research Council of Canada and the CANDU Owners Group are thanked for providing financial support. N. Arbeau, W. Cook and F. Cussac are thanked for their contributions in the laboratory and to the analysis.

**REFERENCES**

Basset, M., Arbeau, N., McInerney, J. and Lister, D.H., 2000 (a), Deposition of Magnetite Particles onto Alloy-800 Steam Generator Tubes, *Proc. 3rd Int. CNS Conference on Steam Generators and Heat Exchangers*.

Basset, M., 1998, Masters Thesis, Department of Chemical Engineering, University of New Brunswick.

Basset, M., McInerney, J., Arbeau, N. and Lister, D.H., 2000 (b), The Fouling of Alloy-800 Heat Exchanger Surfaces by Magnetite Particles, *Can. J. of Chem. Eng*., Vol. 78, No. 1, pp. 40-52.

Beal, S.K., 1970, Deposition of Particles in Turbulent Flow on Channel or Pipe Walls, *Nuclear Science and Engineering*, Vol. 40, pp. 1-11.

Charlesworth, D.H., 1970, The Deposition of Corrosion Products in Boiling Water Systems, *Chemical Engineering Progress Symposium Series*, Vol. 66, No. 104, pp. 21-30.

Cooper, M.G. and Lloyd, A.J.P., 1969, The Microlayer in Nucleate Pool Boiling, *Int. Journal of Heat and Mass Transfer*, Vol. 12, pp. 895 -913.

Epstein, N., 1988, Particulate Fouling of Heat Transfer Surfaces: Mechanisms and Models, *Fouling Science and Technology*, Kluwer Academic Publishers, pp. 143-164.

Hospeti, N.B. and Messler, R.B., 1965, Deposits Formed Beneath Bubbles during Nucleate Boiling of Radioactive Calcium Sulfate Solutions, *AIChE Journal*, Vol. 11, No. 4, pp. 662-665.

Jawurek, H.H., 1969, Simultaneous Determination of Microlayer Geometry and Bubble Growth in Nucleate Boiling, *Int. Journal of Heat and Mass Transfer*, Vol. 12, pp. 843-848.

Kern, D.Q. and Seaton, R.E., 1959, A Theoretical Analysis of Thermal Surface Fouling, *British Chemical Engineering*, Vol. 4, No. 5, pp. 258-262.

McCrea, L., 2001, Masters Thesis, Department of Chemical Engineering, University of New Brunswick.

McNab, G.S. and Meisen, A., 1973, Thermophoresis in Liquids, *Journal of Colloid and Interface Science*, Vol. 44, No. 2, pp. 339-346.

Mizuno, T., Wada, K. and Iwahori, T., 1982, Deposition Rate of Suspended Hematite in a Boiling Water System Under BWR Conditions, *Corrosion-NACE*, Vol. 38, No. 1, pp. 15-19.

Moore, F.D. and Mesler, R.B., 1961, The Measurement of Rapid Surface Temperature Fluctuations during Nucleate Boiling of Water, *AIChE Journal*, Vol. 7, No. 4, pp. 620-624.

Papavergos, P.G. and Hedley, A.B., 1984, Particle Deposition Behaviour from Turbulent Flows, *Chem. Eng. Res. Des*., Vol. 32, pp. 275-295.

Plaza, R.C., Vicente, J., Gomez-Lopera, S. and Delgado, A.V., 2001, Stability of Dispersions of Collodial Nickel Ferrite Spheres, *Journal of Collodial and Interface Science*, Vol. 242, pp.306-313.

Regazzoni, A.E. and Matijevic, E., 1982, Formation of Spherical Colloidal Nickel Ferrite Particles as Model Corrosion Products, *Corrosion-NACE*, Vol. 38, No. 4, pp.212-218.

Robin Jr., T.T. and Snyder, N.W., 1970, Bubble Dynamics in Subcooled Nucleate Boiling Based on the Mass Transfer Mechanism, *Int. Journal of Heat and Mass Transfer*, Vol. 13, pp. 305-318.

Turner, C.W. and Godin, M., 1994, Mechanisms of Magnetite Deposition in Pressurized Boiling and Non-Boiling Water, *Proc. Steam Generator and Heat Exchanger Conference*, Conference Proceedings, Vol. II, Toronto.

Turner, C.W. and Klimas, S.J., 2001, The Effect of Surface Chemistry on Particulate Fouling Under Flow-Boiling Conditions, *Proc. Engineering Foundation Conference on Heat Exchanger Fouling*, Davos, Switzerland.

Turner, C.W., Lister, D.H. and Smith, D.W., 1990, The Deposition and Removal of Submicron Particles of Magnetite at the Surface of Alloy 800, *Proc. Steam Generator and Heat Exchanger Conference*.

Turner, C.W. and Smith, D.W., 1992, A Study of Magnetite Particle Deposition onto Alloy-800 and Alloy-600 Between 25 and 85˚C and Predicted Rates Under Steam Generator Operating Conditions, *Steam Generator Sludge Deposition in Recirculating and Once Through Steam Generator Upper Tube Bundle and Support Plates*, ASME, NE-Vol. 8.